Supplement 1. *Expression of characteristic markers of intercalated cells in outer medullary collecting duct (mOMCD1) cells.* We used mOMCD1 and mIMCD3 cell cultures as the models reminiscent of intercalated cells. We used cultured cells because cAMP measurements in single intercalated cells of the isolated collecting ducts are not yet feasible. To illustrate the suitability of mOMCD1 and mIMCD3 cells as models of the intercalated cells, we examined mRNA and protein expression of anion exchanger 1 (AE1) and vacuolar H^+-ATPase in these cell lines. While H^+-ATPase is expressed in all types of intercalated cells, AE1 is expressed exclusively on the basolateral membrane of the acid-secreting (A-ICs). We have chosen these transporters because mOMCD1 cells were previously demonstrated to actively secrete acid (through H^+-K^+-ATPase and H^+-ATPase) and to increase the rate of acid secretion in response to low media pH,[48] which are functional properties resembling A-ICs.

Supplement 1. Figure S1. *Expression of H^+-ATPase in the cultured collecting duct cells.* **Figure S1a** illustrates RT-PCR of a4 subunit of H^+-ATPase in mOMCD1 and mIMCD3 cells and in the kidney tissue, which was used as a positive control. RT-PCR was performed similarly as described in the Methods section, using the following primer sequences for ATP6V0A4 (GenBank Accession Number: NM_080467): 5'- GAA ACG GCA CGT GGA ATA CT -3' (sense), and 5'- TTG AAG CCA GGT TCC AAA TC -3' (antisense). We used the same primers for β-actin as described in the Methods. H^+-ATPase was detected as a 129 bp band in both mOMCD1 and mIMCD3 cells. **Figure S1b** illustrates H^+-ATPase protein expression detected with indirect immunofluorescence. mOMCD1 cells and tissues were fixed with 4% paraformaldehyde, permeabilized, and incubated with a polyclonal rabbit anti-H^+-ATPase a4 serum (a gift from Carsten Wagner, university of Zurich, Switzerland) used at a dilution 1:200. The labeling was visualized with Alexa Fluor 488 secondary antibodies (Invitrogen, Molecular

Probes, Eugene, OR) used at 1:400 dilution. The cells were also incubated with the nuclear dye Hoechst 33342 (Invitrogen, Molecular Probes, Eugene, OR) at 1:10,000 dilution in order to stain cell nuclei. The labeling was examined and images acquired on the epifluorescent microscope Nikon E600 (Nikon Bioscience, Melville, NY) equipped with SPOT digital camera (Diagnostic Instruments, Sterling Heights, MI). H^+-ATPase labeling was readily detectable in mOMCD1 cells (first panel), where it showed abundant expression in the plasma membrane. The second panel is a differential interference contrast image illustrating the cell shape and membrane position. The labeling was absent in the control slides (third panel) in which the cells were incubated only with the secondary antibody. The positive controls in the kidney tissue (fourth panel) demonstrate the typical apical H^+-ATPase labeling pattern characteristic of A-ICs. (The fluorescent image was merged with differential interference contrast image, which was included to illustrate the tissue morphology.)

Figure S1a.

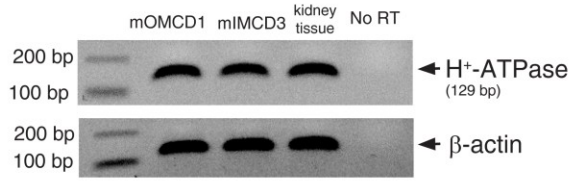

Figure S1b.

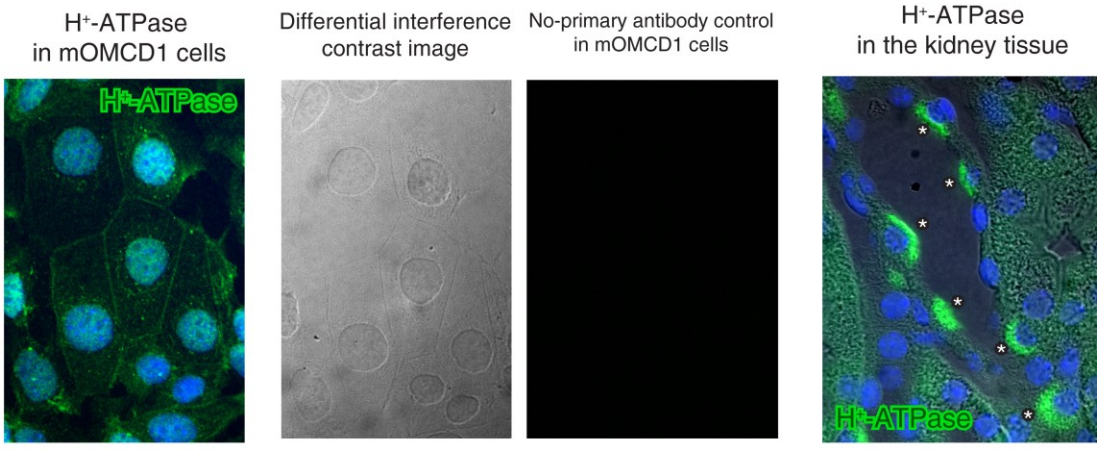

Supplement 1. Figure S2. *Expression of AE1 in the cultured collecting duct cells.* **Figure S2a** illustrates RT-PCR of AE1 mRNA in mOMCD1 and mIMCD3 cells, and in the kidney tissue, which was used as a positive control. RT-PCR was performed similarly as described in the Methods section, using the following primer sequences for AE1 (GenBank Accession Number: AY296129): 5'- GCT CTT CCC ACA GAG CAA AC -3' (sense), and 5'- CTG CCT CCA CCC ATT GTA GT -3' (antisense). We used the same primers for β-actin as described in the Methods. AE1 was detected as a 142 bp band in the mOMCD1 cells and mouse kidney tissue. We were not able however to detect AE1 mRNA in mIMCD3 cells. **Figure S2b** illustrates AE1 protein expression in mOMCD1 cells and in the kidney tissue sections detected with indirect immunofluorescence. Immunocytochemistry was performed and images acquired as is described above (Fig. S1b). Affinity-purified polyclonal rabbit anti-AE1 antibody (Chemicon International, Temecula) was used at the dilution of 1:200. The labeling was visualized with Alexa Fluor 594 secondary antibodies (Invitrogen, Molecular Probes, Eugene, OR) at 1:400 dilution. AE1 labeling was readily detectable in mOMCD1 cells (first panel), with more of the protein located in intracellular vesicles. We have chosen several cells, which were not entirely confluent, because the membrane expression was easier to illustrate in these cells. The second panel shows a differential interference contrast image, illustrating cell shape and membrane position. The labeling was absent from the control slides (third panel) in which it was done without incubation with the primary antibody. The fourth panel demonstrates the typical basolateral AE1 labeling in A-ICs in the kidney tissue sections. (The fluorescent image was merged with differential interference contrast image, which was included to illustrate the tissue morphology.)

Based on these findings, we concluded that mOMCD1 express transport proteins typical of A-ICs, H^+-ATPase and AE1. This finding is consistent with their functional properties described by Gutunpali et al [48] therefore and indicates that mOMCD1 cells can be used a model reminiscent of native intercalated cells.

Figure S1a.

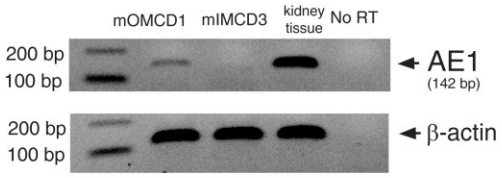

Figure S1b.

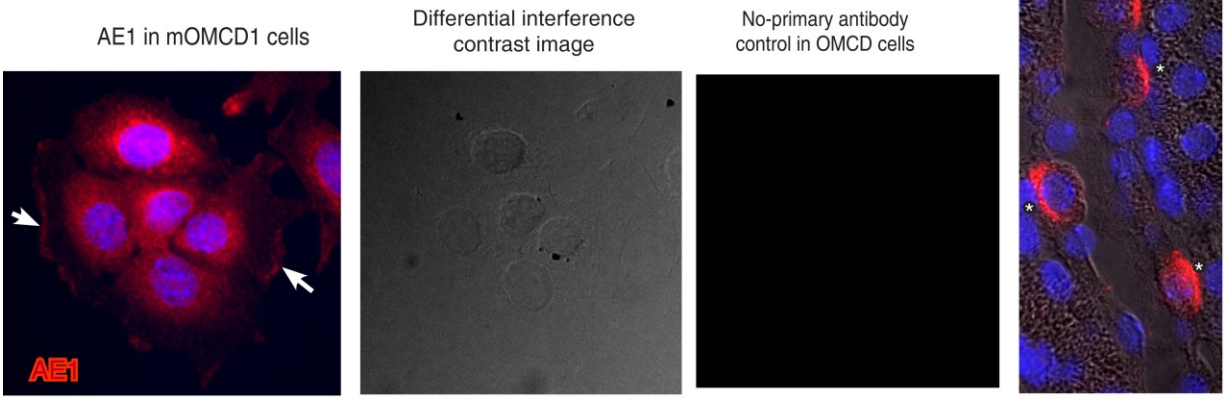

Supplement 2. Figure S3. *Effects of knockdown of HA-GPR4 stably expressed in HEK-293 cells.* HEK-293 cells stably transfected with pcDNA3 vector (Vector) or HA-GPR4 (GPR4) were plated on 60 mm dishes and transfected using Fugene with either 2.6 μg of either missense siRNA (CON) or siRNA targeting GPR4 (Dharmacon). 24h after transfection cells were harvested and plated at a density of $0.5x10^4$ cells/cm^2 into 12 well (for immunoblot analysis) or 48 well dishes (cAMP assay) and grown for 48 h. Cells were then washed and refed serum-free media F12 media pH 8.0 for 6 h, washed again then stimulated with F12 media adjusted to the indicated pH for 10 min in the presence of 1 mM isobutylmethylxanthine (phosphodiesterase inhibitor). cAMP was isolated and quantified by RIA and presented as mean±SD values from 2 experiments (**Fig. S3b**). GPR4 knockdown was assessed by immunoblotting (**Fig. S3a**) using an anti-HA mAb. Basal (pH 8.0) cAMP accumulation was ~3-fold higher in GPR4 CON siRNA vs. Vector CON siRNA cells (0.35 vs. 0.10 pmol/well, respectively), and was ~50% lower in GPR4 siRNA cells (0.18 pmol/well). Forskolin-stimulated cAMP was modestly but not significantly lower (~15%) in GPR4 GPR4 siRNA cells relative to GPR4 CON siRNA cells (not shown).

Figure S3a.

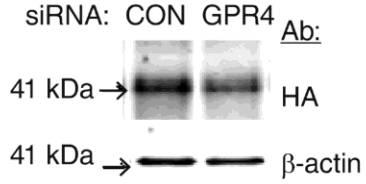

Figure S3b.

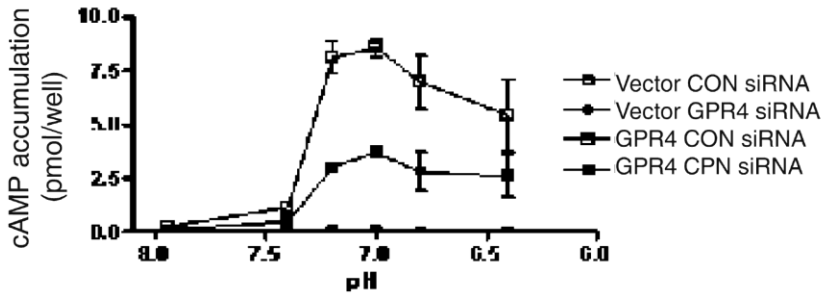

Supplement 3, Figure S4. *Morphology of kidney parenchyma is similar in wild types and GPR4 knockout mice*. Hematoxylin and Eosin (H&E) staining of 4 μm kidney paraffin sections taken from the wild types (panels A, C, and E) and GPR4 knockouts (panels B, D, and F) show normal morphology of the kidney parenchyma in GPR4 knockout mice

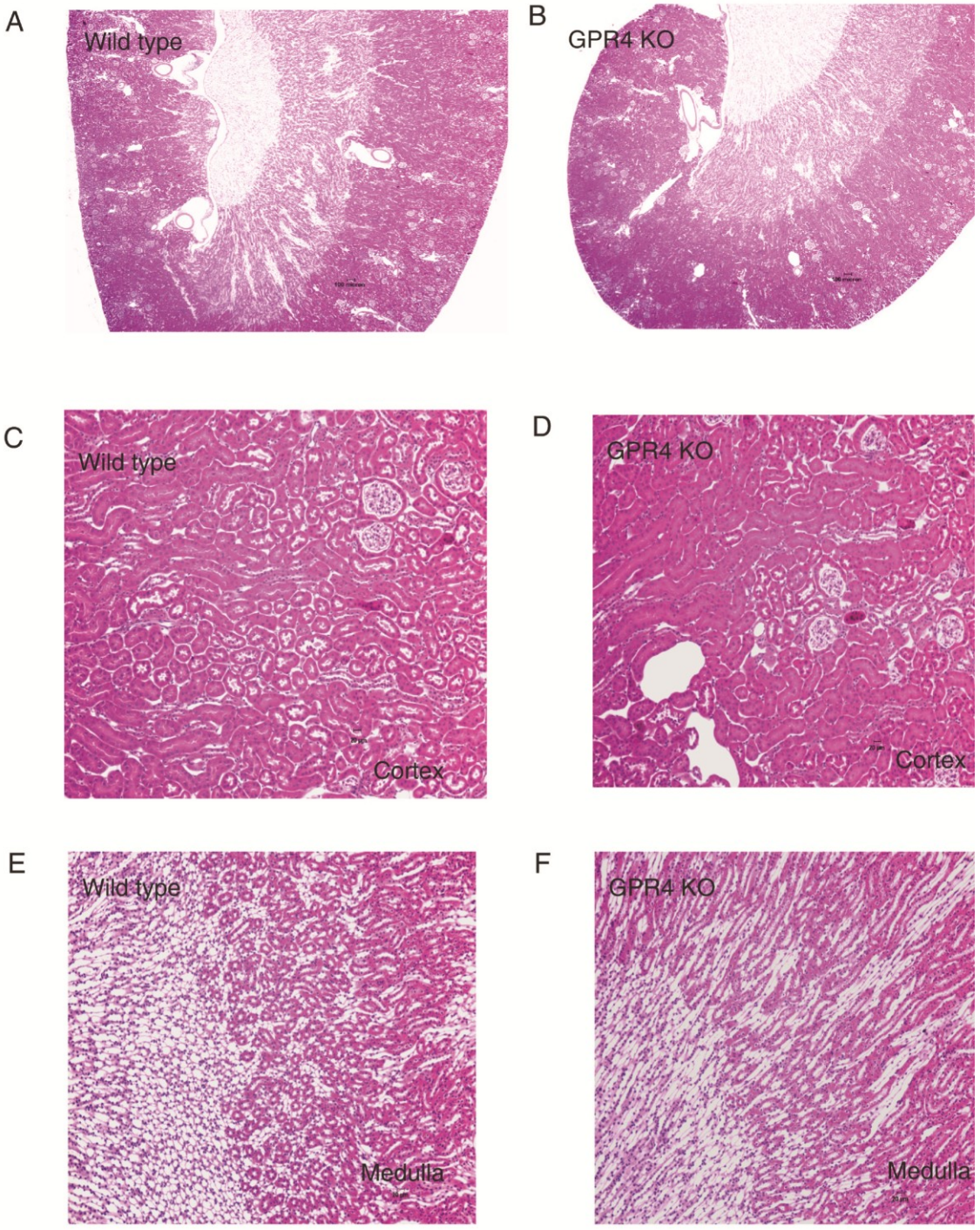

Supplement 3, Figure S5. *Periodic acid-Schiff (PAS) staining does not indicate any expansion of mesangial regions or sclerosis in the kidneys of GPR4 knockouts compared to wild types.* PAS staining of 4 μm kidney paraffin sections is shown in panels A, C, and E (wild types) and in panels B, D, and F (GPR4 knockouts).

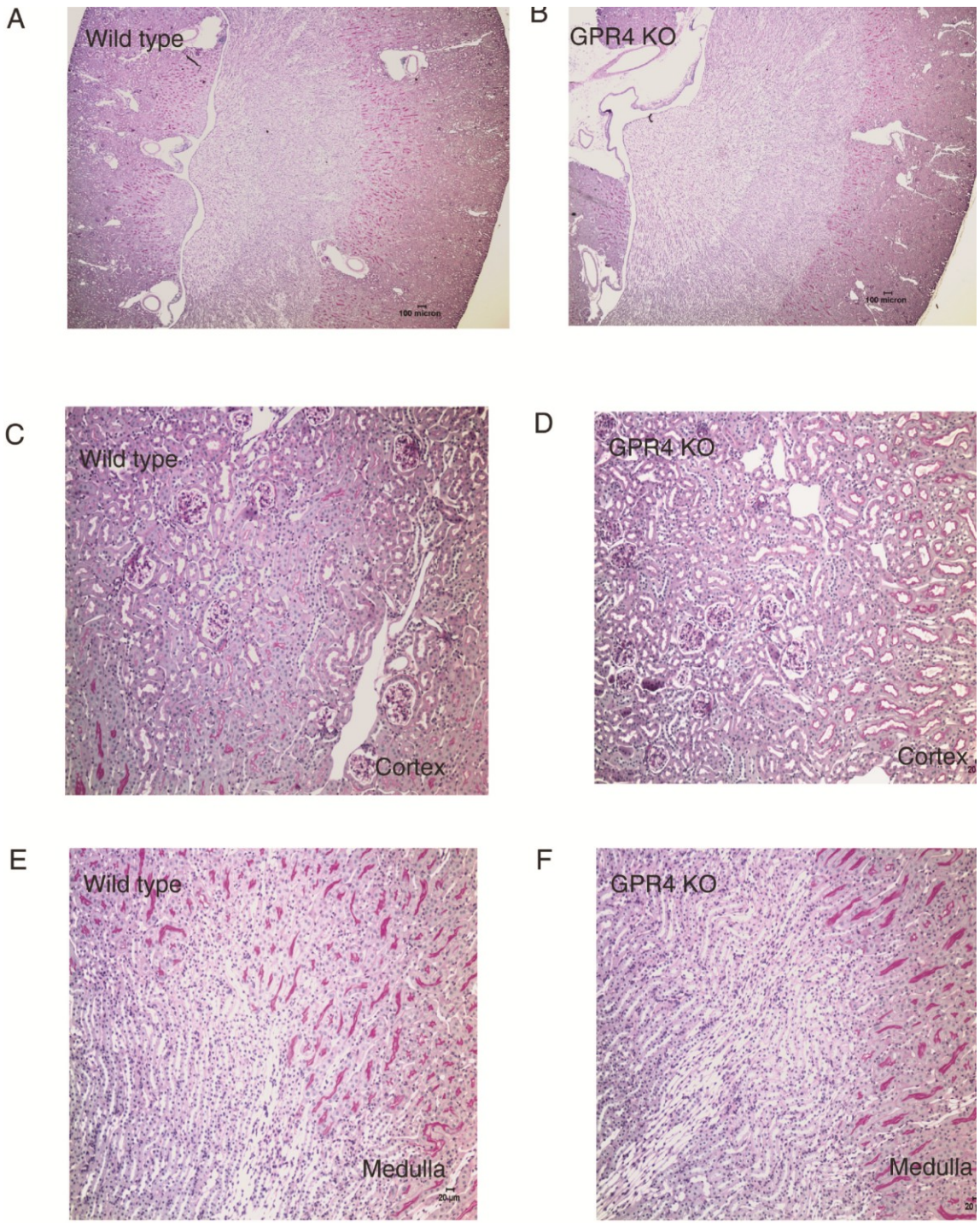

Supplement 3, Figure S6. *Trichrome staining does not indicate any expansion of mesangial regions or sclerosis in the kidneys of GPR4 knockouts compared to wild types.* Trichrome staining of 4 μm kidney paraffin sections is shown in panels A, C, and E (wild types) and in panels B, D, and F (GPR4 knockouts).

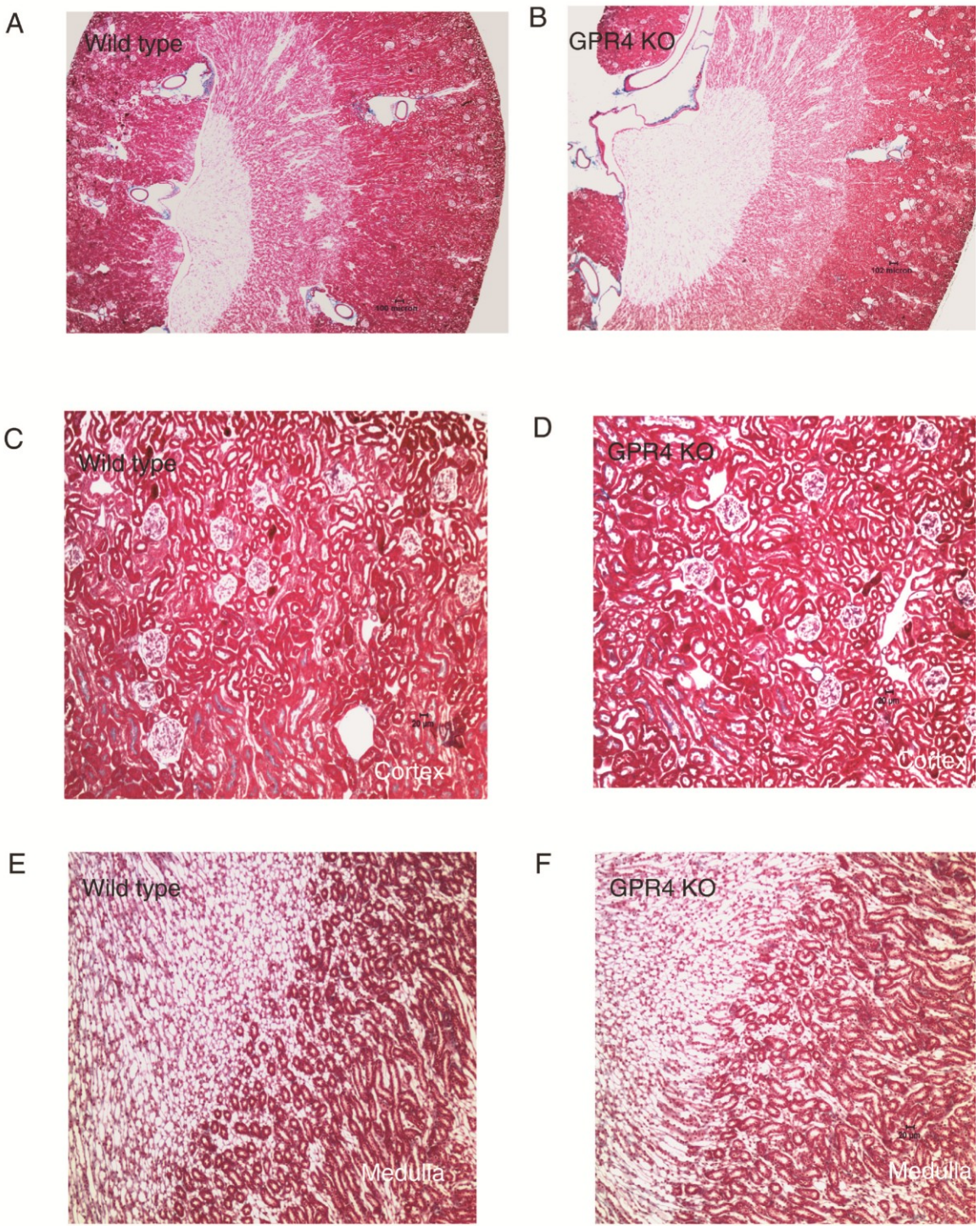

Supplement 4. *Body weight, food and water intake, urine volume, and chloride and sulfate excretion.* Body weight of GPR4-/- and their wild types was comparable: 24.1 ± 0.51 g (n=15) in GPR4-/- vs. 24.9 ± 0.43 g (n=15) in wild types (p=0.27) and so was the intake of food. On average, GPR4-/- consumed 5.06 ± 0.2 g/24h (n=20) and wild types consumed 4.9 ±0.2 g/24h (n=15) (p=0.5). Importantly, food intake corrected for body weight (food intake/body weight) was comparable in knockouts and wild types: 0.21 ± 0.01 in GPR4-/- vs. 0.2 ± 0.01 in wild types, p=0.28. GPR4-/- also drank similar amount of water as the wild types did: GPR4-/- drank 7.53 ± 0.38 ml/24h (n=15) and the wild types 7.07 ± 0.41 ml/24h (n=15). p=0.4. Water intake corrected for body weight (water intake/body weight) was 0.31 ± 0.02 ml/g in GPR4-/- vs. 0.29 ± 0.02 ml/g in wild types (n=15, each), p=0.3. Urine volume in GPR4-/- was 1.12 ± 0.15 ml/24h (n=20) vs. 1.23 ± 0.16 ml/24h (n=15) in wild types (p=0.6).

The intake of food was comparable during acid loading experiments: on average GPR4-/- consumed 5.1 ± 0.3 g/24h and the wild types 5.4 ± 0.2 g/24h (p=0.6). The intake of food corrected for body weight (food intake/body weight) was nearly identical: 0.19 ± 0.01 in GPR4-/- vs. 0.2 ±0.01 (n=10), p=0.3. Similarly, fluid intake corrected for body weight (fluid intake/body weight) was similar: 0.32 ± 0.02 in GPR4-/- vs. 0.3 ± 0.01 in wild types (n=10), p=0.5, indicating comparable acid loading. The intake of fluid reflects acid load, as NH_4Cl is given as 280 mM solution. Since GPR4-/- exhibited lower NEA, it is critical to show that the knockouts did not receive smaller acid load i.e. drank less. In fact, GPR4-/- drank slightly, although not significantly, more (8.6 ± 0.6 ml/24h - GPR4-/- vs. 7.9 ± 0.2 ml/24h - wild types, p=0.3) possibly because they tend to concentrate urine less during acid loading compared to wild types (Table 2). Urine volume was 1.98 ± 0.33 in GPR4-/- vs. 1.63±0.26 in wild types (n=10, each), p=0.4.

NH_4Cl loading also increases chloride in 24h urine. Of note is that urine chloride was identical between GPR4-/- and their wild types, further indicating that the knockouts and wild types received comparable acid load.

Supplement 4. Figure S7. *Urine chloride excretion during acid loading.* Chloride concentration (mmol/L) was measured daily in the urine collected from GPR4-/- and wild types in metabolic cages over 24h period and divided by 24h urine creatinine (mmol/L). The measurements were conducted before acid-loading (baseline) and during subsequent four days of acid loading with 280 mM NH_4Cl in drinking water. The data demonstrate that urine chloride concentration was comparable in GPR4-/- and wild types during acid loading, indicating that knockouts and wild types received comparable acid load.

Figure S7.

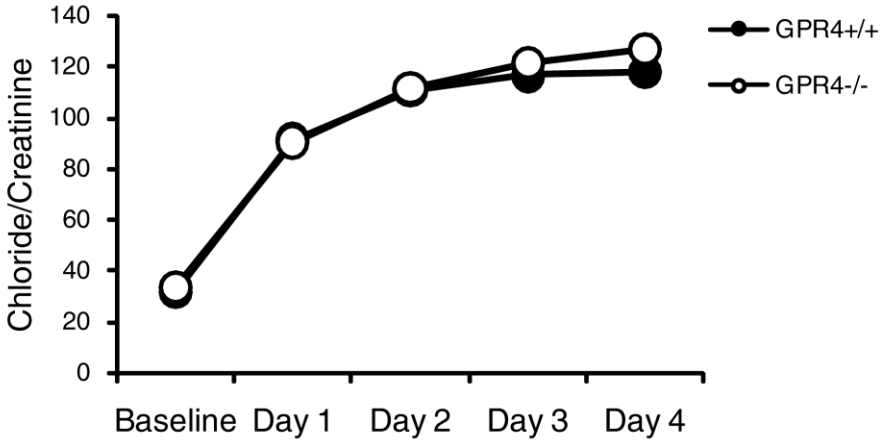

Supplement 4. Figure S8. *Urine sulfate excretion during acid loading.* Sulfate excretion reflects protein content of the diet, so we also measured sulfate in 24h urine samples collected in metabolic cages before and during NH4Cl loading. Urine sulfate excretion showed a tendency to be lower in GPR4-/-, however there was not a significant difference between GPR4-/- and GPR4+/+.

Figure S8.

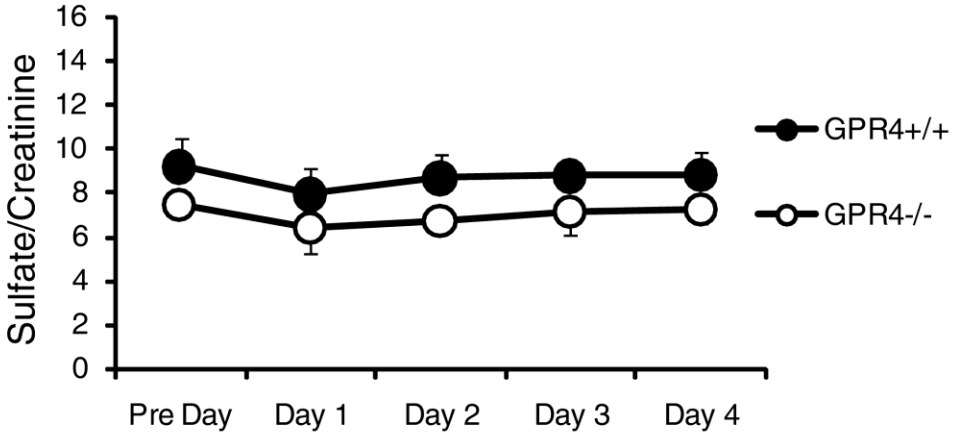

Taken together, these data demonstrate that lower net acid excretion in GPR4-/- was not caused by decreased food or protein intake or lower acid load.

Supplement 5. *Comparison of acid-base status of mice before and after acid loading.*

Table S1. Acid-base and electrolyte status of GPR4 wild type mice (GPR4+/+) at baseline and after acid loading.

Genotype	GPR4+/+	acid loaded GPR4+/+	p values
n	15	10	
Blood			
pH	7.39±0.01	7.35±0.02	0.06
PCO_2	39.6±0.9	33±1.7†††	0.002
PO_2	91.6±4.4	96.5±2	0.4
HCO_3^-	24±0.4	18.3±0.8†††	$1x10^{-6}$
tCO_2	25.1±0.4	19.3±0.8†††	$1x10^{-6}$
K^+	4.8±0.07	5.3±0.06†	0.02
Na^+	146.3±0.9	148.5±1.7	0.1
Cl^-	116.3±1	123±4.5	0.08
iCa^+	1.03±0.06	1.05±0.06	0.7
BEecf	-1.6±0.5	-7.3±1†††	$1x10^{-4}$
Creatinine	0.023±0.002	0.018±0.0007	0.1
BUN	24±1.1	27±3.3	0.2
Urine			
pH	6.08±0.04	5.85±0.03	0.2
Osmolarity	3057±296	4065±152†	0.02
Creatinine	6.7±0.6	4.9±0.1†	0.05
K^+/Creatinine	55.3±2.8	65.5±2.7†	0.03
Na^+/Creatinine	24.3±1.3	31.4±0.8†††	0.002
Cl^-/Creatinine	37.8±1.9	120.6±3.5†††	$2x10^{-10}$
Ca^{2+}/Creatinine	0.14±0.004	0.2±0.01†††	$1x10^{-5}$
$NH4^+$/Creatinine	10.6±0.8	62.6±2†††	$2x10^{-16}$
TA/Creatinine	12.2±0.9	19.8±2.5†††	0.002
NAE/Creatinine	22.6±1.2	82.3±3.4†††	$3x10^{-14}$
NAE	0.19±0.02	0.93±0.03†††	$1x10^{-10}$
Creatinine clearance	0.29±0.02	0.4±0.02†††	0.001

Blood samples were obtained from the tail artery in conscious mice. Urine analyses were performed on samples collected in metabolic cages over 24h period. Urine pH and ammonium measurements were also repeated in fresh urine samples to avoid artifacts associated with the prolonged collection of urine in metabolic cages. Concentrations of electrolytes, creatinine, titratable acids (TA) were expressed in mmol/L, net acid excretion (NAE) in mmol/24h, blood urea nitrogen (BUN) in mg/dl, creatinine clearance in ml/min, osmolarity in mOsmol/L, Pco_2 in mmHg.

† GPR4+/+ vs. acid loaded GPR4+/+: $^{\dagger}p< 0.05$; $^{\dagger\dagger}p<0.01$; $^{\dagger\dagger\dagger}p<0.005$.

Table S2. Acid-base and electrolyte status of GPR4 knockout mice (GPR4-/-) at baseline and after acid loading.

Genotype	GPR4-/-	acid loaded GPR-/-	p values
n	20	10	
Blood			
pH	7.37±0.01	7.32±0.02	0.08
PCO_2	35.7±1.1	34±2.4	0.7
PO_2	92.2±4.7	96.2±4.6	0.6
HCO_3^-	20.3±0.6	$17.8\pm0.5^{\neq\neq}$	0.007
tCO_2	21.7±0.6	$18.8\pm0.5^{\neq\neq}$	0.005
K^+	5.3±0.05	5.4±0.1	0.5
Na^+	145.6±1.1	$150\pm1.1^{\neq\neq}$	0.004
Cl^-	119.4±0.6	$133\pm3.3^{\neq\neq\neq}$	$6x10^{-6}$
iCa^+	1.05±0.03	1.1±0.05	0.09
BEecf	-4.8±0.7	$-7\pm0.4^{\neq}$	0.03
Creatinine	0.025±0.002	$0.018\pm0.0002^{\neq}$	0.01
BUN	26±1.4	29±2	0.2
Urine			
pH	6.37±0.06	$6.0\pm0.07^{\neq}$	0.04
Osmolarity	4220±371	2991±442	0.07
Creatinine	7.9±0.8	$5\pm0.4^{\neq}$	0.02
K^+/Creatinine	54.8±2.9	$65.6\pm1.3^{\neq}$	0.02
Na^+/Creatinine	24.8±1.5	$30.5\pm1.6^{\neq}$	0.03
Cl^-/Creatinine	37.7±1.6	$117.6\pm6.3^{\neq\neq\neq}$	$1x10^{-8}$
Ca^{2+}/Creatinine	0.13±0.003	$0.3\pm0.03^{\neq\neq\neq}$	$1x10^{-8}$
$NH4^+$/Creatinine	8.9±0.6	$44.9\pm4.4^{\neq\neq\neq}$	$1x10^{-11}$
TA/Creatinine	9.7±0.5	$21\pm0.9^{\neq\neq\neq}$	$2x10^{-9}$
NAE/Creatinine	18.4±0.7	$66\pm5.1^{\neq\neq\neq}$	$4x10^{-12}$
NAE	0.14±0.01	$0.66\pm0.03^{\neq\neq\neq}$	$1x10^{-6}$
Creatinine clearance	0.23±0.03	$0.4\pm0.02^{\neq\neq\neq}$	0.001

Blood samples were obtained from the tail artery in conscious mice. Urine analyses were performed on samples collected in metabolic cages over 24h period. Urine pH and ammonium measurements were also repeated in fresh urine samples to avoid artifacts associated with the prolonged collection of urine in metabolic cages. Concentrations of electrolytes, creatinine, titratable acids (TA) were expressed in mmol/L, net acid excretion (NAE) in mmol/24h, blood urea nitrogen (BUN) in mg/dl, creatinine clearance in ml/min, osmolarity in mOsmol/L, Pco_2 in mmHg.

$^{\neq}$ GPR4-/- vs. acid loaded GPR4-/- $^{\neq}p< 0.05$; $^{\neq\neq}p<0.01$; $^{\neq\neq\neq}p<0.005$.

Supplement 6. Figure S9. *Western blot analysis of TRPV5 protein levels in the kidneys of acid loaded GPR-/- and GPR4+/+ mice.* The release of calcium from the bone during metabolic acidosis is accompanied by decreased calcium reabsorption in the kidney. The decreased calcium reabsorption is mediated by decreased expression and activity of the epithelial calcium channel, the transient receptor potential vanilloid channel type 5 (TRPV5) in the kidney and results in concomitant hypercalciuria. This acid load-elicited hypercalciuria is present in GPR4+/+ during acid loading, but is significantly more pronounced in GPR4-/- (Fig. 7). These results prompted us to determine the expression of TRPV5 in the kidney tissue of GPR4-/- and GPR4+/+ mice after four days of acid loading.

One hundred μg of total protein from each sample were resolved with 8-16% Tris-Glycine Gel (Invitrogen, Carlsbad, CA) and transfered to nitrocellulose membranes. The blocked membranes were incubated for 2h with affinity purified polyclonal rabbit anti-TRPV5 antibody (Alomone labs, Jerusalem, Israel) at a dilution of 1:200 or with mouse monoclonal anti-β-actin antibody (Abcam Inc., Cambridge, MA) at a dilution of 1:2500. The antibodies were diluted with 3% nonfat dry milk in TBS-T (20 mM Tris, pH 7.6, 137 mM Sodium Chloride, 0.1% Tween-20). After washing, membranes were incubated for 1h at room temperature with peroxidase-labeled secondary antibodies (KPL, Gaithersburg, MD) diluted 1:5000 in 3% nonfat dry milk in TBS-T. Protein bands on the membranes were developed with 1 Component TMB Membrane Peroxidase Substrate (KPL, Gaithersburg, MD). The anti-TRPV5 antibody recognizes a band of ~ 100 kD and anti-β actin antibody recognizes a band of ~ 42 kD. The immunoblot demonstrates that the expression levels of TRPV5 protein were comparable in kidney tissues harvested from GPR+/+ or GPR4-/- mice.

Figure S9.

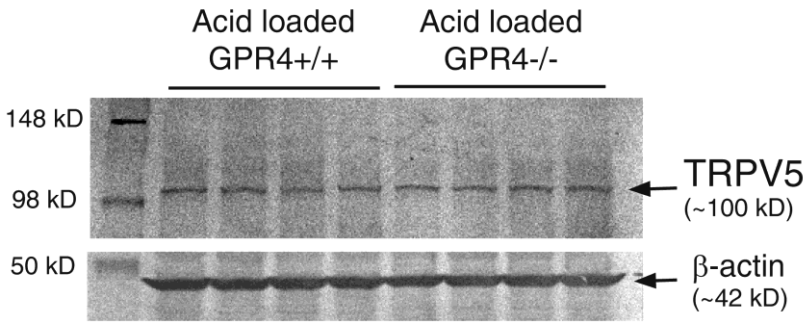
Acid loaded
GPR4+/+
Acid loaded
GPR4-/-
148 kD
98 kD
50 kD
TRPV5
(~100 kD)
β-actin
(~42 kD)